The nuclear chloride ion channel NCC27 is involved in regulation of the cell cycle

Stella M. Valenzuela *, Michele Mazzanti †‡, Raffaella Tonini ‡, Min Ru Qiu *, Kristina Warton *, Elizabeth A. Musgrove §, Terence J. Campbell ‖ and Samuel N. Breit *

*Centre for Immunology, St Vincent's Hospital and The University of New South Wales, Sydney, NSW 2010, Australia, †Dipartimento Biologia Cellulare e dello Sviluppo, Università 'La Sapienza', Roma 00185, ‡Dipartimento Fisiologia e Biochimica Generali, University of Milan, Milan 20133, Italy, ‖Department of Medicine, University of NSW, and Victor Chang Cardiac Research Institute, Sydney, NSW 2010 and §Garvan Institute of Medical Research, Sydney, NSW 2010, Australia

(Received 16 May 2000; accepted after revision 5 August 2000)

1. NCC27 is a nuclear chloride ion channel, identified in the PMA-activated U937 human monocyte cell line. NCC27 mRNA is expressed in virtually all cells and tissues and the gene encoding NCC27 is also highly conserved. Because of these factors, we have examined the hypothesis that NCC27 is involved in cell cycle regulation.

2. Electrophysiological studies in Chinese hamster ovary (CHO-K1) cells indicated that NCC27 chloride conductance varied according to the stage of the cell cycle, being expressed only on the plasma membrane of cells in G2/M phase.

3. We also demonstrate that Cl^- ion channel blockers known to block NCC27 led to arrest of CHO-K1 cells in the G2/M stage of the cell cycle, the same stage at which this ion channel is selectively expressed on the plasma membrane.

4. These data strongly support the hypothesis that NCC27 is involved, in some as yet undetermined manner, in regulation of the cell cycle.

The nucleus is enveloped in a double membrane containing macromolecular pores, through which much nuclear–cytoplasmic transport occurs. Previous paradigms suggested that passive diffusion of ions and small molecules between the nucleus and the cytoplasm occurred through these pores. However, it is now appreciated that the nuclear membrane also contains abundant ion channels. Studies have identified many different types of ion-selective channels in the nuclei of a wide range of cells (Mazzanti *et al.* 1990, 1991; Matzke *et al.* 1990; Tabares *et al.* 1991; Bustamante, 1992; Mak & Foskett, 1994; Pasyk & Foskett, 1995; Rousseau *et al.* 1996; Longin *et al.* 1997) but to date, their physiological role remains unclear. In addition, studies using Ca^{2+}-imaging techniques have demonstrated variations in ion concentrations between the nucleus and cytoplasm (Hernandez-Cruz *et al.* 1990; Przywara *et al.* 1991; Birch *et al.* 1992) and more recently, nuclear Ca^{2+} has been shown to regulate the transport of large molecules through the nuclear pore by inducing the opening and closing of these structures (Perez-Terzic *et al.* 1996; Assandri & Mazzanti, 1997). Speculation as to the role of nuclear ion channels centres around their involvement in regulating ionic traffic between the cytoplasm, nucleoplasm and perinuclear space. By so doing, it is proposed that they could influence nuclear processes ranging from cell proliferation to apoptosis.

Whilst there is substantial evidence for a role of ion channels in cell proliferation and the cell cycle (DeCoursey *et al.* 1984; Gray *et al.* 1986; Chiu & Wilson, 1989; Bubien *et al.* 1990; Deane & Mannie, 1992; Day *et al.* 1993; Wilson & Chiu, 1993; Nilius & Droogmans, 1994; Arcangeli *et al.* 1995; Villaz *et al.* 1995; Ullrich & Sontheimer, 1996, 1997; Chin *et al.* 1997; Pappas & Ritchie, 1998), none of it specifically implicates nuclear ion channels. For example, the activity of a 240 pS K^+ channel has been shown to vary during the cell cycle in pre-implantation mouse embryos. The channel is active throughout M and G1 phases, but no channel activity is detected during the G1-to-S transition (Day *et al.* 1993). Additionally, in human and murine neuroblastoma cell lines, an inwardly rectifying K^+ current has also been shown to be cell cycle regulated. This channel, in turn, regulates the resting potential of these cells (Arcangeli *et al.* 1995).

A number of studies have also demonstrated chloride ion (Cl^-) conductance varying in synchrony with the cell cycle in a number of different cells including freshly isolated human B lymphocytes as well as B- and T-cell lines (Bubien *et al.* 1990). In human glioma cells, expression of a Cl^- current was found to be cell cycle dependent. This current was markedly up-regulated after cell cycle arrest, with the highest Cl^- channel activity in early G1 and the lowest activity in G0/G1 and S phases (Ullrich & Sontheimer, 1997). In ascidian embryos, both cell cycle stage and cell volume (Villaz *et al.* 1995) modulated an inwardly rectifying voltage-gated Cl^- channel. The amplitude of this current varied more than 10-fold during the cell cycle, with the largest amplitude occurring during the exit from M-phase. The authors suggested that this channel may function in membrane trafficking to and from the cell surface. Since membrane is added to the cell surface during both cell swelling and the cell cycle, the appearance of functional Cl^- channels in the plasma membrane under such conditions suggests an essential role in intracellular membranes during the fusion process (Villaz *et al.* 1995).

Further evidence for the involvement of ion channels in the cell cycle has come from studies which show that inhibition of ion channel activity influences cell replication. A variety of classical K^+ channel blockers disrupt mitogenesis in Schwann cells (Chiu & Wilson, 1989; Pappas & Ritchie, 1998), T cells (DeCoursey *et al.* 1984), fibroblasts (Gray *et al.* 1986), tumour cells (Nilius & Droogmans, 1994) and in the astrocytoma cell lines U87 and A172 (Chin *et al.* 1997). Chloride channel blockers have also been associated with changes in cell proliferation. Ullrich & Sontheimer (1996) described a decrease in human astrocytoma proliferation (16·4, 38·2 and 72·6%), following exposure to the Cl^- channel blockers DIDS (200 μM), DNDS (200 μM), as well as Zn^{2+} (200 μM), respectively. However, there was an increase in astrocytoma proliferation upon exposure to another Cl^- channel blocker, chlorotoxin (600 nM). The Cl^- channel blockers SITS and DIDS were found to be effective mitogens and directly stimulated proliferation in cultured B cells (Deane & Mannie, 1992). Similarly, in Schwann cells, exposure to either SITS or DIDS led to a 2- to 5-fold enhancement of proliferation in both unstimulated and mitogen-stimulated cells (Wilson & Chiu, 1993). Ullrich & Sontheimer (1996) proposed that the difference between the actions of the stilbene derivatives such as DIDS and SITS and chlorotoxin may be caused by the former acting upon ion transport mechanisms, while the latter acts as a more specific ion channel inhibitor.

NCC27 is one of the very limited number of cloned nuclear ion channels. It is a 27 kDa protein, which we originally cloned, and characterised from a subtracted cDNA library enriched for macrophage activation associated genes (Valenzuela *et al.* 1997). Whilst NCC27 is unusually small for an ion channel protein, in a recent paper (Tonini *et al.* 2000) we present direct evidence that NCC27 is a transmembrane protein that forms an essential component of an ion channel complex. In this paper we also undertake a detailed electrophysiological characterisation of this ion channel. NCC27 has a high degree of homology to another intracellular Cl^- channel, p64, originally isolated from bovine kidney (Landry *et al.* 1993). Three other closely related ion channels have been described more recently (Duncan *et al.* 1997; Heiss & Poustka, 1997; Qian *et al.* 1999), with the latest member CLIC3, like NCC27, demonstrating a predominantly nuclear localisation. CLIC3 has also been shown to bind a mitogen-activated protein kinase, ERK7, and is suggested to play a role in the regulation of cell growth (Qian *et al.* 1999).

Because of NCC27's nuclear location, wide cellular distribution and high conservation across species, we hypothesised that NCC27 is involved in cell cycle regulation. In this paper we report a series of studies which substantiate a relationship between NCC27 chloride conductance and the cell cycle.

METHODS

Materials

The chloride ion channel blockers used in this study were R(+) IAA-94 (*R*(+)-[(6,7-dichloro-2-cyclopentyl-2,3-dihydro-2-methyl-1-oxo-1H-inden-5yl)-oxy] acetic acid; Biomol Research Laboratories, Inc.), A9C (anthracene-9-carboxylic acid; Sigma) and DIDS (4,4′-diisothiocyanatostilbene-2,2′-disulfonic acid; Sigma).

Cell culture and preparation of transfected cell lines

Cell lines were obtained from the American Type Tissue Collection. Both non-transfected and transfected CHO-K1 cells were grown in DMEM/F12 media (Gibco BRL) containing 5% fetal calf serum (FCS; Gibco BRL).

Eukaryotic expression of NCC27 and NCC27 tagged with the FLAG peptide (DYKDDDDK) at its carboxy terminus was performed as described previously (Valenzuela *et al.* 1997). A construct incorporating a modified FLAG sequence (DYKDDDDN) at the amino terminus of NCC27 was directionally cloned into the pRc/CMV vector (Invitrogen). This construct was transfected into CHO-K1 cells (80% confluent) for 24 h, in 35 mm^2 dishes using 9 μl Lipofectamine Reagent (Life Technologies, Inc.) and 1 μg of DNA, as recommended by the manufacturer. Stable transfectants were selected with G418 (Boehringer Mannheim) followed by subcloning. The subclones were screened by immunofluorescence staining using anti-m2 (anti-FLAG) monoclonal antisera (Sigma) (Valenzuela *et al.* 1997).

The BOSH2BGFP-N1 construct, encoding a histone–GFP fusion protein, was provided by Drs T. Kanda and G. M. Wahl, The Salk Institute for Biological Studies, San Diego, USA (Kanda *et al.* 1998). It contains the blasticidin-S resistance gene originally from Dr F. Hanaoka, Osaka University, Japan. This construct was transfected into monolayers of either control CHO-K1 cells or CHO-K1 cells previously transfected with the amino terminus FLAG-tagged NCC27 construct. The cells (80% confluent) were transfected for 24 h in 35 mm^2 dishes using 9 μl Lipofectamine Reagent and 1 μg of DNA, as recommended by the manufacturer. Stable transfectants were selected with blasticidin-S (Calbiochem) and subclones were then isolated and screened by viewing cells directly under a fluorescence microscope.

PI staining and cell cycle analysis

CHO-K1 cells were seeded at 2×10^5 cells per 25 cm^2 flask in DMEM/F12 media containing 5% FCS. After 24 h, the cells were incubated in the presence or absence of blocker for a further 24 h, after which time all cells (including detached and adherent) were collected, with adherent cells harvested in PBS containing 0·1% EDTA. Cells were then washed twice with PBS, pelleted by centrifugation and resuspended in PBS containing 0·1% Triton X-100, 0·1% BSA, propidium iodide (40 $\mu g\ ml^{-1}$) and RNase A (10 $\mu g\ ml^{-1}$). Samples were then incubated for a minimum of 30 min at 4 °C. The propidium iodide-stained cells were analysed for DNA content on an EPICS XL flow cytometer (Coulter Electronics). Cell cycle analysis was performed using Multicycle software (Phoenix Flow Systems). Results of at least three independent experiments are reported, with values expressed as the percentage difference from subtracted control (percentage of cells in G2/M phase of cell cycle under test condition − percentage under control condition). Controls are CHO-K1 cells exposed to the same concentration of DMSO diluent as the blocker-treated cells. Statistical analyses were performed using ANOVA (STATVIEW program).

Northern blots

Commercially obtained Northern blot membranes (2 μg of polyA^+ RNA per lane) (Clontech) were probed with the entire cDNA encoding NCC27, labelled with [γ-^{32}P]dCTP using the Megaprime Labelling Kit (Amersham) or with a 28S rRNA oligonucleotide (TCCGTCCGTCGTCCTCCTC) end-labelled with [α-^{32}P]ATP. Hybridisation was overnight at 65 °C, with the final wash in 0·1% SSPE–0·1% SDS for 5 min. Blots were exposed using XAR-5 X-ray film (Eastman Kodak Co.) with Cronex Lightening Plus intensifying screens (Dupont) at −70 °C.

Patch-clamp recording

The patch electrodes were pulled from hard borosilicate glass (Hilgenberg) on a Brown-Flaming P-87 puller (Sutter Instruments). The pipettes were coated with Sylgard (Dow Corning) and fire polished to an external tip diameter of 1–1·5 μm. These electrodes had resistances of 7–10 MΩ. We applied standard cell-attached and nucleus-attached patch-clamp techniques to obtain seals of 20–50 GΩ in the single-channel recordings. The bath solution for the CHO-K1 cells contained (mM): 130 NaCl, 4·8 KCl, 1·2 $MgCl_2$, 1 $CaCl_2$, 10 Hepes, 12·5 glucose and 1·2 NaH_2PO_4. For cell-attached and inside-out recordings, the same solution was used in the micropipettes. For single-channel outside-out experiments, the patch electrode solution contained (mM): 10 NaCl, 130 potassium aspartate, 2 $MgCl_2$, 1·3 $CaCl_2$, 10 Hepes and 10 EGTA. The antibody (m2-mab, Sigma) was applied at a concentration of 1·5 $\mu g\ ml^{-1}$ in the bath solution for whole-cell recording using a custom-made fast perfusion system. Whole-cell patch electrodes were filled with (mM): 140 KCl, 1·2 $MgCl_2$, 10 Hepes and 5 EGTA. Chloride channel blockers (IAA-94, A9C and DIDS) were used at a concentration of 10 μM. Single-channel and whole-cell currents were recorded with an Axopatch 200B (Axon Instruments) patch-clamp amplifier and were digitised and stored on a personal computer using commercial software (pCLAMP 7, Axon Instruments). All whole-cell current traces were not leakage subtracted. Data were analysed after filtering at 1000 Hz using custom-made programs developed by W. Gooldby (Department of Anatomy and Cell Biology, Emory University, Atlanta, GA, USA). All electrophysiological data are shown in the figures as means ± 1 S.E.M.

RESULTS

NCC27 is encoded by a widely expressed and highly conserved gene

In order to examine the distribution of NCC27 mRNA, human adult and fetal tissue Northern blots were probed using the entire cDNA insert encoding NCC27 (Fig. 1*A*). All Northern blots were also probed with a 2 kB human β-actin cDNA probe as a control to ensure even loading of mRNA in all tracks (results not shown). As described previously, NCC27 cDNA detects two mRNA transcripts, which we believe represent alternate transcripts (Valenzuela *et al.* 1997). NCC27 mRNA was expressed in virtually all of the fetal and adult human tissues studied. It was, however, only detected at relatively low levels in fetal brain, with adult brain and skeletal muscle showing even lower levels. Northern blots of various mouse tissues yielded similar results (Fig. 1*B*). In mouse embryos, expression levels of NCC27 mRNA did not vary from day 7 to 17, indicating that the

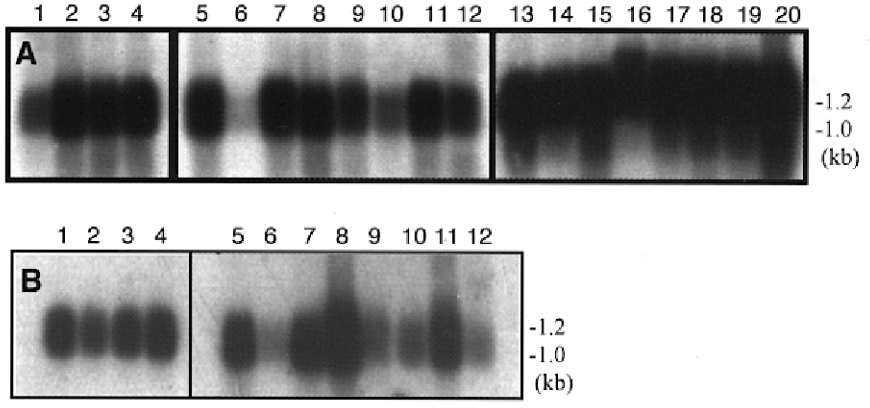

Figure 1. Northern blots of whole tissues probed with NCC27 cDNA

A, human fetal tissue: (1) brain, (2) lung, (3) liver, (4) kidney; human adult tissue: (5) heart, (6) brain, (7) placenta, (8) lung, (9) liver, (10) skeletal muscle, (11) kidney, (12) pancreas (13) spleen, (14) thymus, (15) prostate, (16) testis, (17) ovary, (18) small intestine, (19) colon, (20) peripheral blood leucocyte. *B*, whole mouse embryos: (1) day 7 (2) day 11 (3) day 15 (4) day 17; mouse tissue: (5) heart, (6) brain, (7) spleen, (8) lung, (9) liver, (10) skeletal muscle, (11) kidney, (12) testis.

gene is active from a very early stage in embryogenesis through to adult life. The distribution of NCC27 mRNA therefore appears to be virtually ubiquitous, suggesting that it is likely to play some basic biological function common to most, if not all, cells.

NCC27 is a member of a family of intracellular ion channel proteins

The first member of this family to be described was a 437 amino acid protein, p64 (L16547), originally isolated from bovine kidney tissue (Landry *et al.* 1993). A homologue of p64 was isolated from rat brain tissue, and designated p64H1 (Duncan *et al.* 1997). NCC27 (U93205), isolated from the human monocyte cell line U937, is a much smaller protein than p64, containing only 241 amino acids. Another related human gene has also been identified, which encodes a 243 amino acid protein CLIC2 (Y12696) (Heiss & Poustka, 1997) and more recently CLIC3 (AF102166) (Qian *et al.* 1999). NCC27 shares 63% identity with bovine p64, 61% identity with human CLIC2, 66% with rat p64H1 and 49% identity with human CLIC3.

The NCC27 gene is highly conserved across species. Southern blot analysis (not shown) indicates that the NCC27 cDNA probe cross hybridises with genomic DNA from all the eukaryotic species studied, which included monkey, rat, mouse, dog, cow, rabbit and yeast. Furthermore, NCC27 shares 90–100% identity to a growing number of human, rat and mouse expressed sequence tags (EST). It is also 99·1% identical over 109 amino acids to a porcine EST

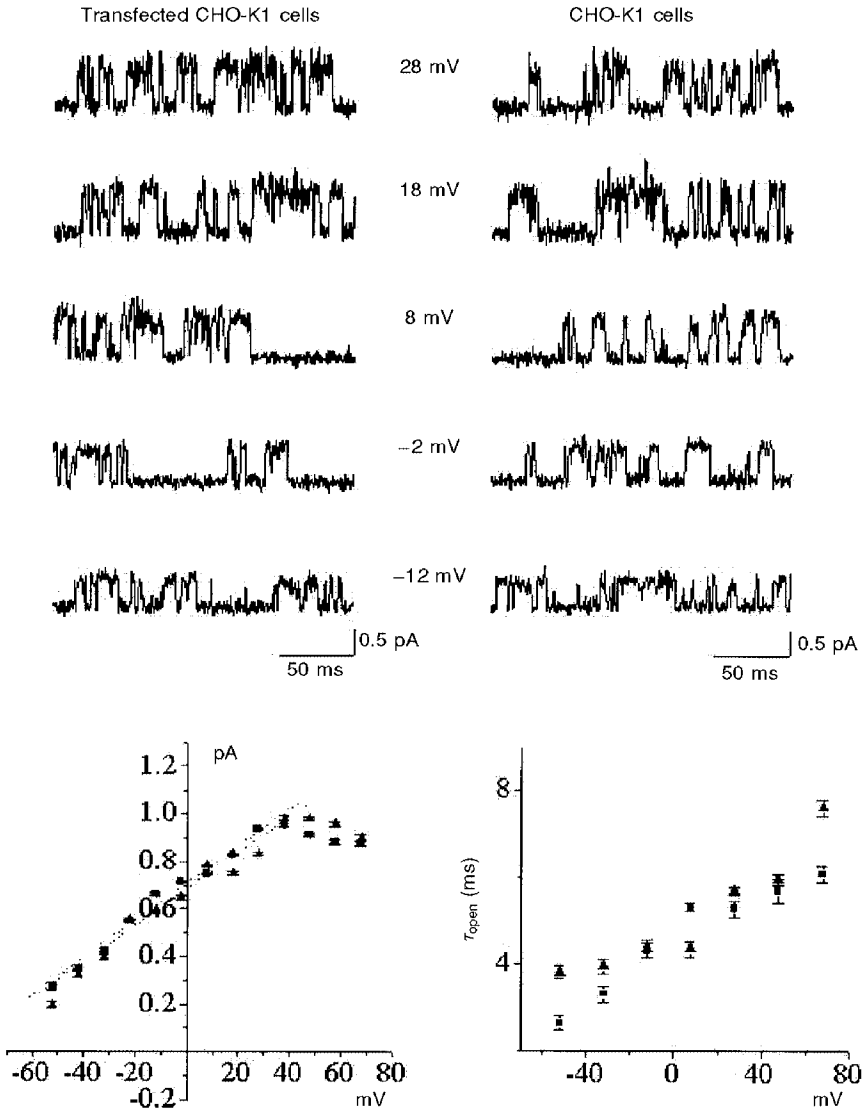

Figure 2. Comparison of channel properties from NCC27-transfected CHO-K1 cells and untransfected CHO-K1 cells

The upper panels are single-channel current traces recorded at different membrane potentials from NCC27-transfected (left) and untransfected (right) CHO-K1 cells. The lower panels show current–voltage (i–V) relationships (left) and channel open times (right), derived from 500 ms of data at each potential (▲, transfected cells; ■, untransfected cells). The biophysical properties of the channel obtained from the two cell types appear to be identical (see text).

(SSC24B10) and 63·4 % identical over 152 amino acids to an EST from zebrafish (AA497337). This strong sequence conservation across disparate species in conjunction with its extremely wide tissue distribution once more supports the argument for its essential role in the biology of the cell.

NCC27 channels transfected into CHO-K1 cells display identical electrophysiological characteristics to an endogenous channel found in untransfected CHO-K1 cells

NCC27 Cl^- conductance was first characterised by us, using CHO-K1 cells transfected with the eukaryotic expression vector pRc/CMV containing the cDNA encoding NCC27. In that first report, we noted that we had found abundant evidence of NCC27 channel activity on both the plasma and nuclear membranes of NCC27-transfected CHO-K1 cells, but only on the nuclear membrane of non-transfected CHO-K1 cells (Valenzuela *et al.* 1997). However, the NCC27 protein can be detected in non-transfected CHO-K1 cells using both immunofluorescence and Western blotting (Valenzuela *et al.* 1997).

Since then, we have undertaken further single-channel recordings on the plasma membrane of both non-transfected and NCC27-transfected CHO-K1 cells. We have confirmed that NCC27 is abundantly expressed on the plasma membrane of transfected cells (we recorded such activity in $> 25\%$ of 50 patches in these cells), but have also found channels which very closely resemble it in 3 out of 80 patches obtained on non-transfected cells (Tonini *et al.* 2000).

Figure 2 is a detailed comparison of the single-channel characteristics of this activity, recorded in both control and NCC27-transfected CHO-K1 cells. These data were pooled from a total of nine successful experiments in NCC27-transfected CHO-K1 cells ($n = 50$ cells), and three successful patches recorded from non-transfected CHO-K1 cells ($n = 80$ cells). Both channels exhibit similar chloride selectivity (Valenzuela *et al.* 1997), and the single-channel characteristics in both cell types could not be separated statistically (Fig. 2). It can be seen from this figure that their i–V curves (bottom, left panel) were essentially the same over the range of potentials studied, and showed identical slope conductances and non-linearities at more positive voltages. Comparison of the linear regression of the two curves gives a significance of $P = 0{\cdot}7$. The single-channel conductance for the transfected cell recordings was $7{\cdot}76 \pm 0{\cdot}47$ pS (mean of 3 separate patches), and for the three recordings we were able to obtain from non-transfected cells, it was $7{\cdot}82 \pm 0{\cdot}39$ pS. The mean open times were also the same over a wide range of potentials. Comparison of the linear regression of these two curves gives a significance of $P = 0{\cdot}5$.

Thus transfection of the NCC27 gene into CHO-K1 cells results in the expression of a Cl^- conductance, which behaves in a similar manner to an endogenous Cl^- conductance detected in CHO-K1 cells. However, the endogenous NCC27 Cl^- conductance detectable on the plasma membrane is only expressed at very low levels, at least under the conditions of this study.

It is possible to visually identify CHO-K1 cells in the G2/M phase of the cell cycle

CHO-K1 cells grow as an adherent monolayer and, under phase contrast microscopy, it is possible to identify morphological differences characteristic of various stages of the cell cycle. Adherent cells in G2/M phase undergo changes in their cytoskeleton that cause them to round up from the tissue culture dish, becoming only loosely adherent and spherical in appearance. Cells in G1 or S phase on the other hand remain spread out and firmly adherent to the tissue culture dish (Alberts *et al.* 1994). In order to confirm the identity of individual cells in G2/M, non-transfected and amino terminus FLAG-tagged NCC27-transfected CHO-K1 cells were transfected with a gene encoding a histone–GFP fusion protein (BOSH2B-GFP) (Kanda *et al.* 1998). Stably transfected cells were isolated by selection with blasticidin-S. Binding of the GFP-labelled histone results in the fluorescence labelling of chromosomes in living cells (Kanda *et al.* 1998). From Fig. 3 it is clear that the cells which by phase contrast microscopy appeared round and detached from the monolayer surface (Fig. 3*B*), were in fact those cells which were undergoing mitosis (Fig. 3*A*–*C*).

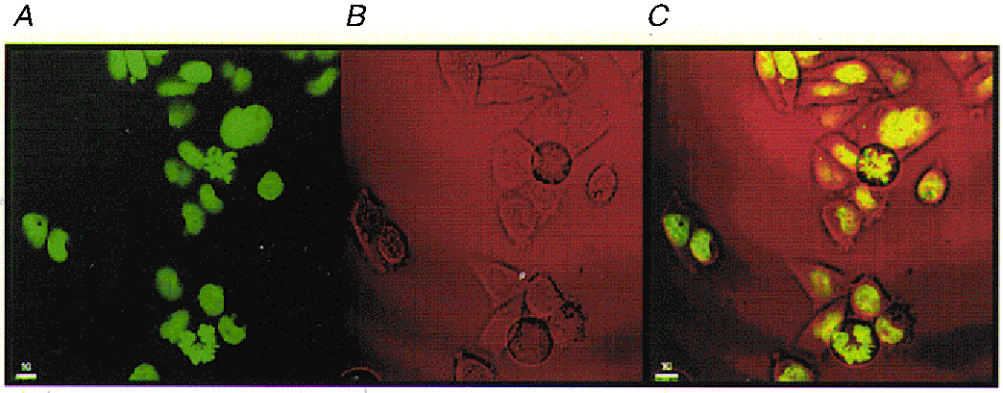

Figure 3. CHO-K1 cells expressing a histone–GFP fusion protein

Photograph of CHO-K1 cells expressing a histone–GFP fusion protein as viewed under fluorescence microscopy (*A*), phase contrast microscopy (*B*) and an overlay of images from *A* and *B* (*C*).

NCC27 Cl^- conductance is found on the plasma membrane of normal CHO-K1 cells only in G2/M phase of the cell cycle

Figure 4 illustrates that in NCC27-transfected CHO-K1 cells under whole-cell voltage clamp conditions, the total voltage-dependent current density was almost twice as high in round (G2/M phase) cells, as it was in flat (G1/S phase) cells. The whole-cell currents illustrated in Fig. 4*A* have not been leakage subtracted. However, comparison of the whole-cell *I–V* relationships from round *versus* flat cells (Fig. 4*A* and *B*, left and right panels) shows that increases in current were mainly due to higher functional expression of NCC27 in round cells. In Fig. 4*C*, we show experiments using the inside-out configuration on transfected CHO-K1 cells. The patch pipette and the bath contained the same solution, which was the same solution as was used in the pipette of whole-cell experiments (above) in order to reproduce at a single-channel level the same conditions as those of the whole-cell measurements. The top panel of Fig. 4*C* shows a macropatch current and its relationship. The lower panel depicts current averages ($n = 4$ each curve) of single-channel recordings obtained at different test potentials. The patch contained only one channel which demonstrated all the same characteristics of NCC27 chloride conductance. From the current kinetics and the *i–V* relationships of the inside-out experiment we suggest that the increments of the current density visible in round cells compared with flat cells are mainly due to the higher presence of NCC27 conductances.

Furthermore, we were able to confirm that in NCC27-transfected CHO-K1 cells, the majority of the current was, in fact, due to the NCC27 channel by use of a specific antibody used to block the chloride current, discussed in the next section (see Fig. 6).

Identical protocols in non-transfected CHO-K1 cells also showed increased whole-cell conductance in the round cell type compared with the flat cells, but in this case the

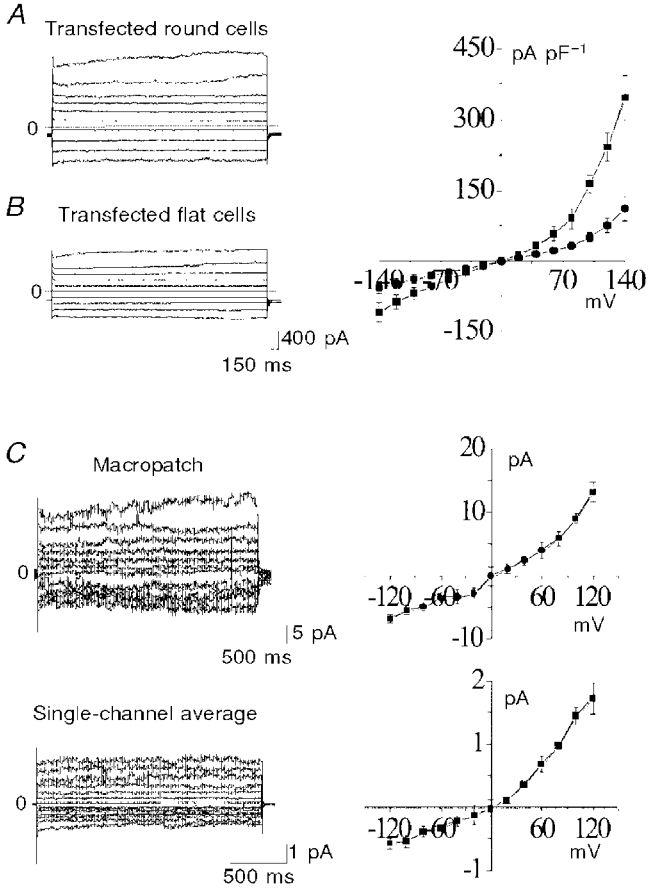

Figure 4

A and *B*, whole-cell patch-clamp recordings of NCC27-transfected CHO-K1 cells from either round (*A*) or flat (*B*) cells. Current amplitudes were measured at 350 ms from the voltage step onset. The current amplitude was 60% greater in round cells (*A*) than in flat cells (*B*). The *I–V* relationships differ between the cell types (top right panel: ■, round cells; ●, flat cells). *C*, inside-out experiments using macropatch configuration (top) and single-channel recording (bottom), both done using similar transmembrane chloride concentrations to those present in the whole-cell studies. The lower *i–V* curve plots the averages obtained from all four such patches in which only a single channel was present. The single-channel *i–V* relationships are very similar to those in the whole-cell recordings from round cells (above), consistent with the hypothesis that NCC27 is responsible for the current increment seen in round cells.

contrast was far greater, with minimal or no current being recorded from untransfected, flat CHO-K1 cells (Fig. 5). This latter finding is consistent with our earlier observation that NCC27-like channel activity is virtually absent from non-transfected flat CHO-K1 cells. Most flat cells, in fact, express no detectable current. Only occasionally were we able to record a (very small) current from flat cells (Fig. 5, inset). It thus appears that endogenous NCC27 Cl^- channels are present to a significant extent in the plasma membrane of CHO-K1 cells only during G2/M phase. Significant NCC27 current is seen in transfected cells in G1/S phase (although still much less than that seen in G2/M phase in the same cells). Thus virtually all of the NCC27 Cl^- channel activity detected in the plasma membrane of flat (G1/S), transfected CHO-K1 cells is carried by the transfected recombinant protein.

Confirmation of this latter point can be seen in Fig. 6 in which we used CHO-K1 cells transfected with NCC27 tagged at its amino terminus with the eight amino acid FLAG epitope, following a previously described approach (Tonini *et al.* 2000). Whole-cell currents (similar to those illustrated in Fig. 4) were reduced by an average of 65% ($n = 5$) after 3–8 min exposure to a monoclonal antibody against the FLAG epitope. Subtraction of the pre- and post-monoclonal antibody whole-cell currents revealed the pure NCC27 component of the control whole-cell current (Fig. 6, lower panel). Use of a class-matched irrelevant monoclonal antibody showed no effect (data not shown).

Cell shape alone does not determine NCC27 plasma membrane Cl^- conductance of control CHO-K1 cells

To exclude the possibility that the changes we observed in NCC27 conductance were due purely to changes in cell shape rather than to the phase of the cell cycle, we induced rounding up of flat cells, without change in their cycle status, by the addition of 2 mM EDTA. We performed these experiments in six non-transfected, flat CHO-K1 cells and in five transfected, flat CHO-K1 cells. In all cases the cells rounded up without any change whatsoever in the recorded whole-cell currents (data not shown).

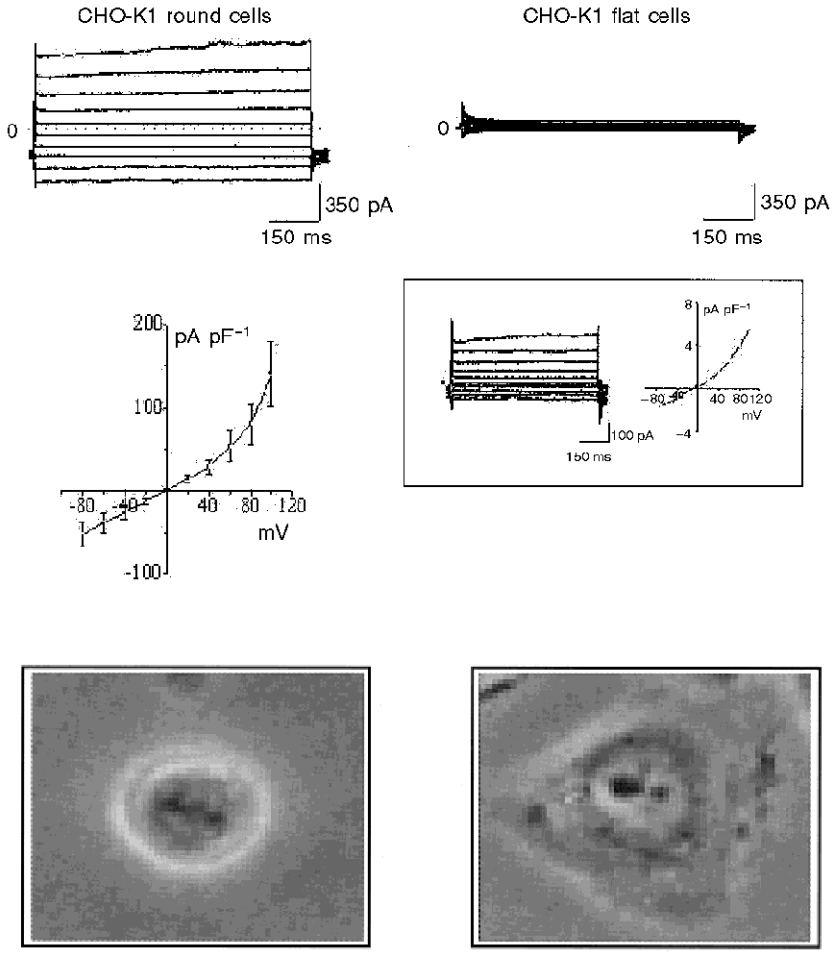

Figure 5. Comparison of whole-cell currents recorded from round, i.e. dividing ($n = 8$; left), and flat, i.e. non-dividing ($n = 8$; right), untransfected CHO-K1 cells

The flat cells have markedly less current than the round cells on average, although 4–5% of flat cells exhibit similar currents to those seen in all round cells (see inset on the right). The similarity of the *I–V* plots (middle left and inset on the right) also suggest the presence of the same channel. Bottom panels show micrographs of round (left) and flat (right) cells as viewed under a phase contrast microscope.

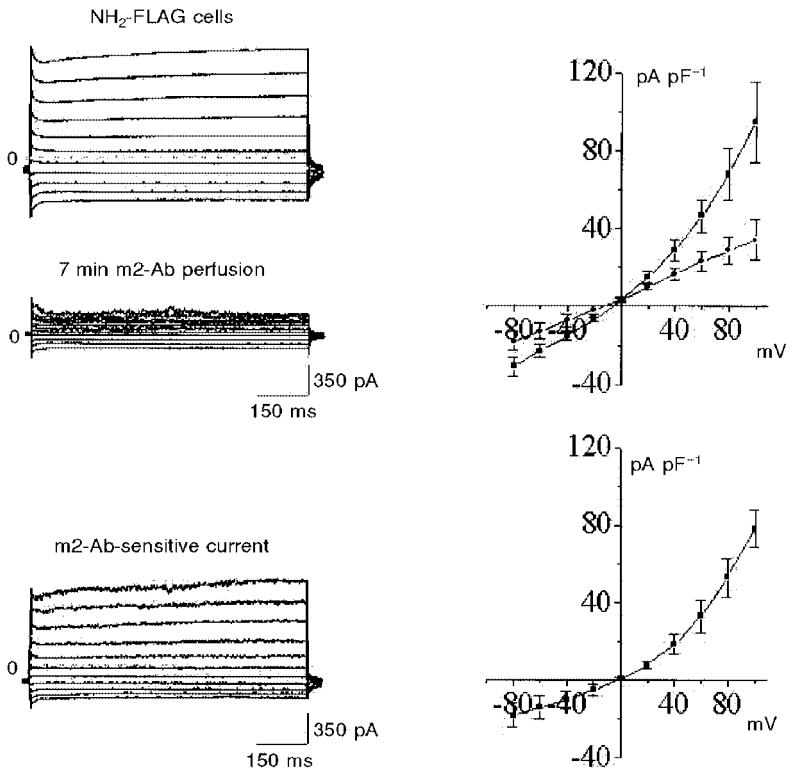

Figure 6. Effect of anti-FLAG m2 monoclonal antibody on the whole-cell current of amino terminal FLAG-transfected NCC27 cells ($n = 5$)

The two upper left panels show currents from the same cell before (top) and 7 min after (bottom) exposure to m2 antibody. The *I–V* curves on the top right show combined results for 5 such experiments (■, control; ●, after exposure to m2 antibody). Both inward and particularly outward currents are markedly reduced by m2 antibody, without a shift in the reversal potential. The bottom left traces are the m2 antibody-sensitive component of current (derived by subtracting the two records above). The *I–V* curve for this antibody-sensitive current (lower right) closely resembles that recorded from untransfected round CHO-K1 cells (Fig. 5).

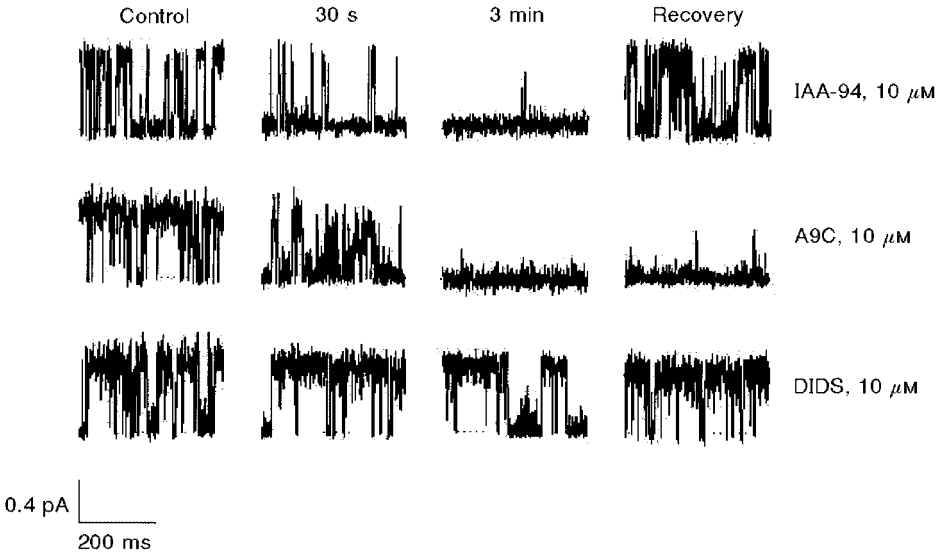

Figure 7. Effects of chloride ion channel blockers on single-channel NCC27 currents

The top panel demonstrates the effect of IAA-94. Current blockade begins within 30 s and is complete at 3 min, but recovers fully and rapidly. A9C (middle panel) produces rapid, complete but irreversible block. DIDS had no effect on the NCC27 single-channel current (bottom panel).

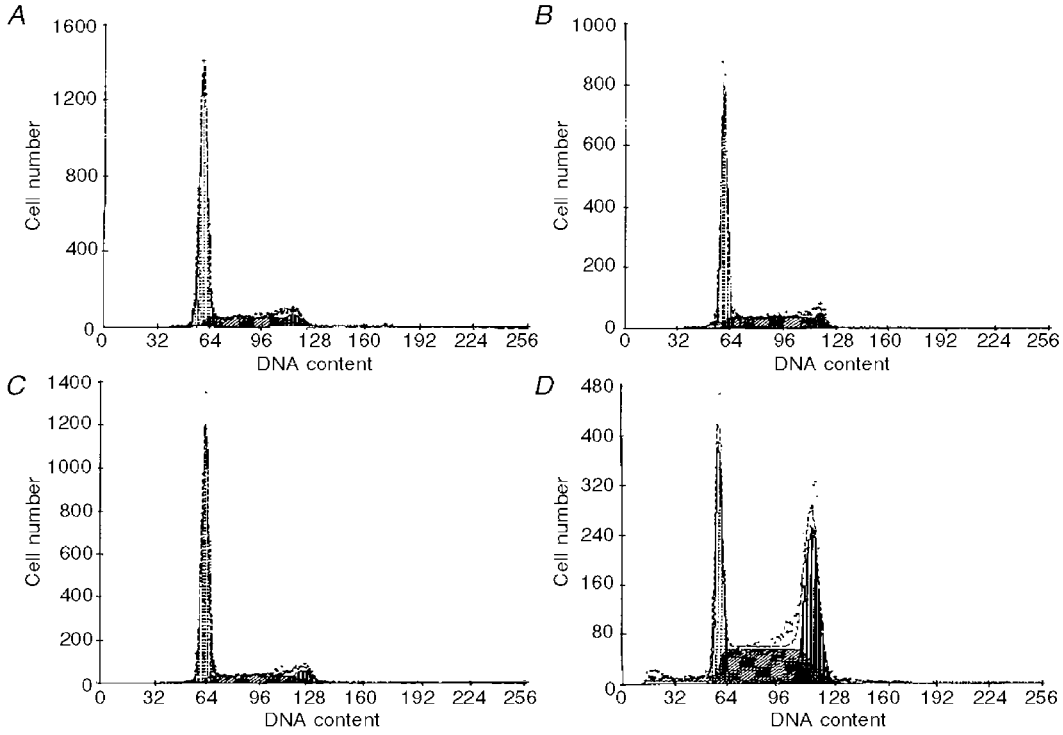

Figure 8. Histograms showing relative distribution of DNA content (*x*-axis) from CHO-K1 cells (cell number, *y*-axis)

Untreated control (*A*), DMSO control (*B*), 1 mM DIDS (*C*) and 1 mM IAA-94 (*D*).

NCC27 ion channel is blocked by IAA-94 and A9C but not DIDS

We studied the effects of a range of pharmacological Cl^- channel blockers on the NCC27 conductance. Single-channel recordings were made in the outside-out configuration. IAA-94 completely and reversibly blocked NCC27 channel currents with a rapid time course (Fig. 7). A9C also completely blocked this current, although more slowly, and the block did not reverse after several minutes of washout in control solution. In contrast, DIDS had no effect (Fig. 7).

Blocking of the NCC27 ion channel arrests replication of CHO-K1 cells at G2/M phase of the cell cycle

In this series of experiments we studied the effects of the blockers reported above on the cell cycle distribution of CHO-K1 cells. We incubated replicating CHO-K1 cells for 24 h with IAA-94, A9C or DIDS at varying concentrations. We used propidium iodide staining and flow cytometric analysis to assess the percentage of cells in the G2/M phase of the cycle. Exposure to IAA-94 (Fig. 8) and A9C produced an increase in the proportion of normal CHO-K1 cells

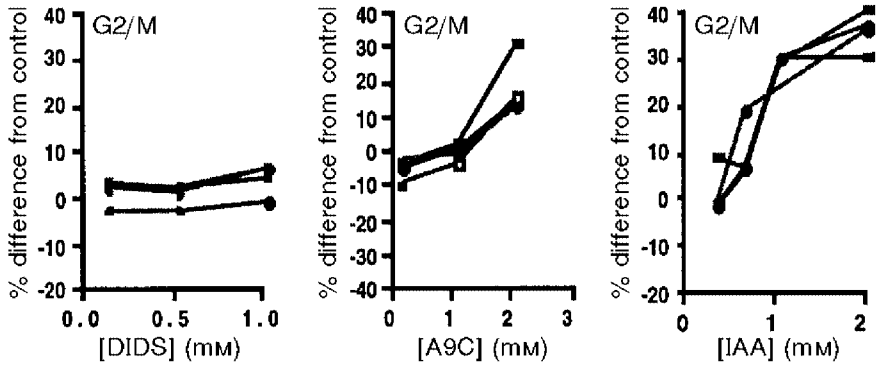

Figure 9. Line graphs from 3 independent experiments demonstrating the effects of increasing concentrations of Cl^- channel blockers on the proportion of CHO-K1 cells in G2/M phase (expressed as % change from control)

DIDS had no effect at any concentration (left). A9C significantly increased the fraction in G2/M at 2 mM ($P < 0{\cdot}0003$), but not at 1 mM. IAA-94 produced a dose-dependent increase at all concentrations studied ($P < 0{\cdot}0001$), with the effect appearing to plateau above 1 mM.

arrested in the G2/M phase of the cycle. This difference between G2/M percentages of control and treated cells was calculated by subtracting the percentage of cells in G2/M phase of the control sample from the percentage of cells in G2/M phase of the blocker-treated sample. It went from $-0{\cdot}6 \pm 5{\cdot}2$ to $33{\cdot}7 \pm 4{\cdot}3\%$ for 2 mM IAA-94 and from $-8{\cdot}2 \pm 3{\cdot}1$ to $15{\cdot}9 \pm 8{\cdot}4\%$ for 2 mM A9C, and was statistically significant (Fig. 9). In contrast, DIDS, which does not block the NCC27 conductance, had no discernible effect in these studies, going from $-0{\cdot}7 \pm 2{\cdot}5$ to $2{\cdot}1 \pm 3{\cdot}5\%$ for 1 mM DIDS (Fig. 9). Thus both IAA-94 and A9C growth arrested a large percentage of replicating CHO-K1 cells in the G2/M stage of the cell cycle. This is also the stage at which NCC27 is expressed on the plasma membrane of CHO-K1 cells.

Whilst we found that the concentration of the blockers required to influence cell cycle progression in this way was well above the IC_{50}, as determined from our patch-clamp data, this is consistent with previous reports on the concentration-dependent inhibition of proliferation and K^+ currents (Wonderlin & Strobl, 1996). The need to use higher concentrations of blockers during the cell cycle experiments than in the patch-clamp studies may be attributed to factors such as the binding of the blockers to serum present in the culture medium, non-specific binding to culture vessels, as well as their possible metabolism and degradation over the 24 h incubation period. Such events could markedly reduce the effective blocker concentrations (Wonderlin & Strobl, 1996). In addition, whilst blocker data should be viewed critically on the grounds of uncertain specificity, in the context of the other available information, our results are consistent with a role for NCC27 in the cell cycle.

DISCUSSION

Although the precise function of NCC27 remains unclear, various factors led us to examine its role in the cell cycle. Firstly, mRNA encoding NCC27 is expressed in virtually all tissues and cells studied to date from various species. In addition the gene is highly conserved across species, ranging from humans and zebrafish, to yeast. When taken together with the predominantly nuclear localisation of NCC27 in CHO-K1 cells this suggests that NCC27 participates in some basic biological process common to most cells.

We believe our observation that, in native CHO-K1 cells, NCC27 Cl^- conductance occurs only during the G2/M phase of the cell cycle, constitutes strong evidence for a role for NCC27 in the cell cycle. A possible interpretation we offer is as follows. In higher eukaryotic cells, the nuclear envelope is completely disassembled during mitosis. In non-transfected CHO-K1 cells the bulk of the NCC27 protein is located in the nucleoplasm, with small amounts also present in the cytoplasm and on the nuclear envelope. Upon dissolution of the nuclear envelope, free soluble NCC27 from the nucleoplasm 'spills' into the cytoplasm, increasing the soluble cytoplasmic pool of NCC27. This allows excess protein to escape regulatory mechanisms which normally prevent its integration into the plasma membrane. We propose that NCC27 may play a role in cytokinesis at the plasma membrane, and dissolution and/or reformation of the nuclear membrane during mitosis, by regulating 'swelling' of both the cell and nucleus, leading to the subsequent division of the former or pinching off into vesicles of the latter. Involvement of Cl^- channels and Cl^- ions in vesicular swelling required for exocytosis and secretion has been well documented in the literature (Jena *et al.* 1997). Furthermore, ion channel involvement in the cell cycle may provide the means by which cells couple changes in cell volume to the cell cycle (Villaz *et al.* 1995).

In addition to these observations, we have demonstrated that the Cl^- channel blockers IAA-94 and A9C inhibit NCC27 Cl^- conductance. Upon exposure of normal CHO-K1 cells to these blockers we demonstrate accumulation of cells in G2/M phase of the cell cycle, the phase during which NCC27 is located on the plasma membrane. We therefore propose that blocking the channel has the effect of preventing cells from completing mitosis, possibly by preventing NCC27-mediated changes in cell volume, which in turn may prevent the cells from physically dividing and/or prevent dissolution of the nuclear envelope. Similarly, disruption of NCC27 function in ionic Cl^- regulation may prevent other downstream events and thus cell cycle checkpoint mechanisms prevent the cell from completing mitosis.

Alberts, B., Bray, D., Lewis, J., Raff, M., Roberts, K. & Watson, J. D. (1994). *Molecular Biology of the Cell*, pp. 863–910. Garland Publishing, Inc., New York and London.

Arcangeli, A., Bianchi, L., Becchetti, A., Favarelli, L., Coronnello, M., Mini, E., Olivotto, M. & Wanke, E. (1995). A novel inward-rectifying K^+ current with a cell-cycle dependence governs the resting potential of mammalian neuroblastoma cells. *Journal of Physiology* **489**, 455–471.

Assandri, R. & Mazzanti, M. (1997). Ionic permeability on isolated mouse liver nuclei: influence of ATP and Ca^{2+}. *Journal of Membrane Biology* **157**, 301–309.

Birch, B. D., Eng, D. L. & Kocsis, J. D. (1992). Intranuclear Ca^{2+} transients during neurite regeneration of an adult mammalian neuron. *Proceedings of the National Academy of Sciences of the USA* **89**, 7978–7982.

Bubien, J. K., Kirk, K. L., Rado, T. A. & Frizzell, R. A. (1990). Cell cycle dependence of chloride permeability in normal and cystic fibrosis lymphocytes. *Science* **248**, 1416–1419.

Bustamante, J. O. (1992). Nuclear ion channels in cardiac myocytes. *Pflügers Archiv* **421**, 473–485.

Chin, L. S., Park, C. C., Zitnay, K. M., Sinha, M., DiPatri, A. J. Jr, Perillan, P. & Simard, J. M. (1997). 4-Aminopyridine causes apoptosis and blocks an outward rectifier K^+ channel in malignant astrocytoma cell lines. *Journal of Neuroscience Research* **48**, 122–127.

Chiu, S. Y. & Wilson, G. F. (1989). The role of potassium channels in Schwann cell proliferation in Wallerian degeneration of explant rabbit sciatic nerves. *Journal of Physiology* **408**, 199–222.

Day, M. L., Pickering, S. J., Johnson, M. H. & Cook, D. I. (1993). Cell-cycle control of a large-conductance K^+ channel in mouse early embryos. *Nature* **365**, 560–562.

Deane, K. H. & Mannie, M. D. (1992). An alternative pathway of B cell activation: stilbene disulfonates interact with a Cl^- binding motif on AEn-related proteins to stimulate mitogenesis. *European Journal of Immunology* **22**, 1165–1171.

DeCoursey, T. E., Chandy, K. G., Gupta, S. & Cahalan, M. D. (1984). Voltage-gated K^+ channels in human T lymphocytes: a role in mitogenesis? *Nature* **307**, 465–468.

Duncan, R. R., Westwood, P. K., Boyd, A. & Ashley, R. H. (1997). Rat brain p64H1, expression of a new member of the p64 chloride channel protein family in endoplasmic reticulum. *Journal of Biological Chemistry* **272**, 23880–23886.

Gray, P. T. A., Chiu, S. Y., Bevan, S. & Ritchie, J. M. (1986). Ion channels in rabbit cultured fibroblasts. *Proceedings of the Royal Society* B **227**, 1–16.

Heiss, N. S. & Poustka, A. (1997). Genomic structure of a novel chloride channel gene, CLIC2, in Xq28. *Genomics* **45**, 224–228.

Hernandez-Cruz, A., Sala, F. & Adams, P. R. (1990). Subcellular calcium transients visualized by confocal microscopy in a voltage-clamped vertebrate neuron. *Science* **247**, 858–862.

Jena, B. P., Schneider, S. W., Geibel, J. P., Webster, P., Oberleithner, H. & Sritharan, K. C. (1997). Gi regulation of secretory vesicle swelling examined by atomic force microscopy. *Proceedings of the National Academy of Sciences of the USA* **94**, 13317–13322.

Kanda, T., Sullivan, K. F. & Wahl, G. M. (1998). Histone-GFP fusion protein enables sensitive analysis of chromosome dynamics in living mammalian cells. *Current Biology* **8**, 377–385.

Landry, D., Sullivan, S., Nicholaides, M., Redhead, C., Edelman, A., Field, M., Al-Awqati, Q. & Edwards, J. (1993). Molecular cloning and characterization of p64, a chloride channel protein from kidney microsomes. *Journal of Biological Chemistry* **268**, 14948–14955.

Longin, A.-S., Mezin, P., Favier, A. & Verdetti, J. (1997). Presence of zinc and calcium permeant channels in the inner membrane of the nuclear envelope. *Biochemical and Biophysical Research Communications* **235**, 236–241.

Mak, D. O. D. & Foskett, J. K. (1994). Single-channel inositol 1,4,5-triphosphate receptor currents revealed by patch clamp of isolated *Xenopus* oocyte nuclei. *Journal of Biological Chemistry* **269**, 29375–29378.

Matzke, A. J. M., Weiger, T. M. & Matzke, M. A. (1990). Detection of a large cation-sensitive channel in nuclear envelopes of avian erythrocytes. *FEBS Letters* **271**, 161–164.

Mazzanti, M., DeFelice, L. J., Cohen, J. & Malter, H. (1990). Ion channels in the nuclear envelope. *Nature* **343**, 764–767.

Mazzanti, M., DeFelice, L. J. & Smith, E. F. (1991). Ion channels in murine nuclei during early development and in fully differentiated adult cells. *Journal of Membrane Biology* **121**, 189–198.

Nilius, B. & Droogmans, G. (1994). A role for K^+ channels in cell proliferation. *News in Physiological Sciences* **9**, 105–110.

Pappas, C. A. & Ritchie, J. M. (1998). Effect of specific ion channel blockers on cultured Schwann cell proliferation. *Glia* **22**, 113–120.

Pasyk, E. A. & Foskett, J. K. (1995). Mutant (ΔF508) cystic fibrosis transmembrane conductance regulator Cl^- channel is functional when retained in the endoplasmic reticulum of mammalian cells. *Journal of Biological Chemistry* **270**, 12347–12350.

Perez-Terzic, C., Pyle, J., Jaconi, M., Stehno-Bittel, L. & Clapham, D. E. (1996). Conformational states of the nuclear pore complex induced by depletion of nuclear Ca^{2+} stores. *Science* **273**, 1875–1877.

Przywara, D. A., Bhave, S. V., Bhave, A., Wakade, T. D. & Wakade, A. R. (1991). Stimulated rise in neuronal calcium is faster and greater in the nucleus than the cytosol. *FASEB Journal* **5**, 217–222.

Qian, Z., Okuhara, D., Abe, M. K. & Rosner, M. R. (1999). Molecular cloning and characterization of a mitogen-activated protein kinase-associated intracellular chloride channel. *Journal of Biological Chemistry* **274**, 1621–1627.

Rousseau, E., Michaud, C., Lefebvre, D., Proteau, S. & Decrouy, A. (1996). Reconstitution of ionic channels from inner and outer membranes of mammalian cardiac nuclei. *Biophysical Journal* **70**, 703–714.

Tabares, L., Mazzanti, M. & Clapham, D. E. (1991). Chloride channels in the nuclear membrane. *Journal of Membrane Biology* **123**, 49–54.

Tonini, R., Ferroni, A., Valenzuela, S. M., Warton, K., Campbell, T. J., Breit, S. N. & Mazzanti, M. (2000). Characterisation of the NCC27 nuclear chloride ion channel: comparison of its electrophysiological properties on the nuclear and plasma membranes and inhibition of its conductance in transfected CHO-K1 cells by antibody blockade. *FASEB Journal* **14**, 1171–1178.

Ullrich, N. & Sontheimer, H. (1996). Biophysical and pharmacological characterisation of chloride currents in human astrocytoma cells. *American Journal of Physiology* **270**, C1511–1521.

Ullrich, N. & Sontheimer, H. (1997). Cell cycle-dependent expression of a glioma-specific chloride current: proposed link to cytoskeletal changes. *American Journal of Physiology* **273**, C1290–1297.

Valenzuela, S.-M., Martin, D. K., Por, S. B., Robbins, J. M., Warton, K., Bootcov, M. R., Schofield, P. R., Campbell, T. J. & Breit, S. N. (1997). Molecular cloning and expression of a chloride ion channel of cell nuclei. *Journal of Biological Chemistry* **272**, 12575–12582.

Villaz, M., Cinniger, J. C. & Moody, W. J. (1995). A voltage-gated chloride channel in ascidian embryos modulated by both cell cycle clock and cell volume. *Journal of Physiology* **488**, 689–699.

Wilson, G. F. & Chiu, S. Y. (1993). Mitogenic factors regulate ion channels in Schwann cells cultured from newborn rat sciatic nerve. *Journal of Physiology* **470**, 501–520.

Wonderlin, W. F. & Strobl, J. S. (1996). Potassium channels, proliferation and G1 progression. *Journal of Membrane Biology* **154**, 91–107.

Acknowledgements

This work was funded in part by Meriton Apartments Pty Ltd through a research and development syndicate arranged by Macquarie Bank Limited, by a NSW Health Research and Development Infrastructure grant, by the Italian Ministry of Research MURST and by the National Research Council (CNR). We thank Virginia Nink and John Zaunders for their assistance with the flow cytometric analysis.

Corresponding author

S. N. Breit: Centre for Immunology, St Vincent's Hospital, Cnr Boundary and West Streets, Sydney, NSW 2010, Australia.

Email: s.breit@cfi.unsw.edu.au

Author's present address

S. M. Valenzuela: School of Pathology, The University of New South Wales, Sydney, NSW 2052, Australia.

Email: stella@unsw.edu.au